

Glucose Sensors Based on Chitosan Capped ZnS Doped Mn Nanomaterials

Son Hai Nguyen¹, Phan Kim Thi Vu², and Mai Thi Tran²

¹School of Mechanical Engineering, Hanoi University of Science and Technology, Hanoi 100000, Vietnam

Manuscript received 19 December 2022; revised 20 January 2023; accepted 25 January 2023. Date of publication 27 January 2023; date of current version 8 February 2023.

Abstract—A typical glucose sensor is a glucose oxidase (GOx) enzyme-based sensor due to its high sensitivity and selectivity. However, it has difficulty activating and stabilizing the enzyme. To enhance the stability of GOx-based sensors, chitosan is added to ZnS-doped Mn nanoparticles. Chitosan stabilizes the ZnS-doped Mn particles and can induce charge processes such as creation, transfer, and separation at the polymer interface and nanoparticles' interface. Hence, it is a strong candidate for electrochemical glucose sensing applications. This letter reports the impedance biosensor based on ZnS-doped Mn-capped chitosan nanomaterials and microinterdigitated electrodes. The glucose sensors' high sensitivity, accuracy, and stability are obtained in the range of 2 to 10 mM. In addition, an application of the Canny edge detection to enhance the limit of detection is demonstrated using experimental data.

Index Terms—Chemical and biological sensors, biosensor, edge detection, glucose, the limit of detection (LOD).

I. INTRODUCTION

Glucose is a critical source of cells and blood. It contributes as an essential energy source to cellular metabolism and the natural growth of cells. Either glucose deficiency or excess can induce a detrimental effect on the functioning of the cells. Especially high glucose levels in the blood or urine can cause diabetes [1], [2], [3]. On the other hand, low glucose levels can cause permanent brain damage [4]. For fast diagnosis and control of diabetes, biosensors have been developed to measure the basic glucose level. The standard method for glucose sensing is enzyme-based sensors. In general, researchers use the enzyme glucose oxidase (GOx) to enhance the sensitivity and selectivity of glucose sensing [4]. However, the enzymatic sensors have some limitations in activating and stabilizing the enzyme. The performance of these sensors also relies on many factors, such as temperature, humidity, pH, etc., that are not always easy to control [5], [6]. To enhance the stability, we use a polymer named Chitosan as a catalytic material to stabilize and improve the number of moving charges. Chitosan-capped Mn-ZnS nanoparticles are commonly used for optical biosensors due to their excellent emitting, stable, and nontoxic properties [7]. For example, Sharma et al. [7] investigated the feasibility of using CH-capped Mn-dopped ZnS nanoparticles for glucose sensing applications based on photoluminescence changes. Wang [8] described a fluorescent sensor for detecting iodine ions based on a CH-ZnS/Mn composite film. Hwang [9] presented his research on CH-ZnS/Mn nanocrystals as sensing materials for fluorescent sensors to detect copper (II) ions in aqueous solutions. However, to the authors' knowledge, there is no report on using these materials for electrochemical glucose sensing.

Electrical impedance spectroscopy (EIS) is an ideal method to monitor glucose levels continuously and promptly [10], [11]. The resistance and reactance values are quantified by measuring the complex impedance changing to the applied frequency and glucose concentration. Each component's resistance/capacitance/inductance in a Randles cell indicates various electrochemical properties. Given an

Corresponding author: Mai Thi Tran (e-mail: maidhbkhn@gmail.com). Associate Editor: K. Shankar. Digital Object Identifier 10.1109/LSENS.2023.3240240

arbitrary electrochemical cell that is suitably modeled by a Randles cell [12], a Nyquist plot is obtained. As a result, a relationship between the effectiveness resistance and glucose concentration can be determined. In our experiment, this relationship can be approximated by a linear function for a range of 2 to 10 mM glucose.

In many practical applications, when glucose concentration is deficient, such as in saliva or tears, detecting the small change in glucose level is difficult. Here, we adapt the Canny edge detector [13] to find the transition between glucose levels in our experiment. This approach can be applied to any signal change needing impedance and other applications, such as Quartz crystal microbalance.

II. METHOD

A. ZnS-Doped Mn Preparations

In this letter, we used the chemicals without any further purification as follows: Zinc acetate dihydrate $Zn(CH_3COO)_2.2H_2O$ (99.99%, Merck, Germany); Sodium sulfide nonahydrate $Na_2S.9H_2O$ (98%, China); Manganese chloride tetrahydrate $MnCl_2.4H_2O$ (99.99%, Merck, Germany); Chitosan $(C_6H_{11}NO_4)n$ (90%, China); Acid acetic (CH₃COOH) (100%, Merk, Germany); Ethanol (C₂H₅OH) (99.9%, China); and distilled water.

B. Synthesis of Chitosan Capped ZnS/Mn (CH-ZnS/Mn) Nanomaterials

Chitosan-capped ZnS-doped Mn (CH-ZnS/Mn) nanomaterials were prepared by the chemical co-precipitation method [14]. In this letter, Zinc acetate and Sodium sulfide, both 0.5M, were mixed with a ratio of 9.0:1.0. For all the tests of this letter, we used 2.0 wt % of Chitosan as a capping agent. First, we added 8.78 g Zinc acetate dihydrate and 0.08 g Manganese chloride tetrahydrate into 80 mL deionized water and stirred the mixture for 30 mins at room temperature to create the suspension A. Meanwhile, 0.5 g Chitosan (CH) was dissolved entirely with 40 mL acid acetic 1%wt to have suspension B. Suspension B was mixed with suspension A to have the final mixture of 2.0 wt% of chitosan. Then we gradually dropped the 2.4 g Sodium sulfide into

²College of Engineering and Computer Science, VinUniversity, Hanoi 100000, Vietnam

Fig. 1. Schematic and parameters of the indigitated electrodes.

the mixture and mixed them for 2 h. After that, the precipitation was collected by centrifuging at 4000 r/min for 5 mins and washed five times using Ethanol. The powder was dried in a vacuum oven at 60 $^{\circ}\text{C}$ for a day.

C. Interdigitated-Electrodes Design and Glucose Test Using EIS Measurements

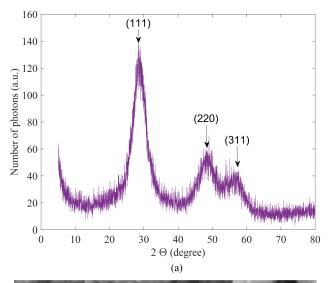
The interdigitated electrode (IDE) design and the parameters are shown in Fig. 1. The IDEs have a comb-liked shape which includes 20 fingers, a gap size of 200 μm , and a finger's width of 400 μm . The electrodes are made of aluminum coated with lead. This simple design is easily and fast prepared at a low cost. Bard et al. [15] first described the advantages of the IDEs are that they do not need a redox electrode and label the sensing film. The IDE-based sensor works as an electrochemical transducer to detect the slight variation in resistance or capacitance of various analytes. In our study, we use electrochemical impedance spectroscopy to observe the behaviors of the sensor and measure the electric signals quantitatively to the amount and concentrations of glucose solutions with frequency.

In our experiments, the electrodes were cleaned with Ethanol, then spin-coated with 100 μl of the mixture of GOx and CH-ZnS/Mn nanomaterials. We prepared the mixture by adding 125 mg GOx into 1L distilled water. When GOx was dissolved completely, we added 2.5 g CH-capped ZnS-doped Mn into the suspension. The thickness of the sensing film was controlled by the spin coating speed at 1500 r/min for 30 s. The film was dried at room temperature for a few hours. Electrochemical characterization was conducted using the Hioki LCR IM3536. The dc voltage was set to 10 mV, ensuring the working domain was linear. The frequency was scanned from 10 to 10 kHz. The impedance and the phase difference are acquired to explore the chemical binding effects of glucose on the electrode surfaces in real time. We also investigated how the sensor performed at 10 Hz when a different amount of glucose was applied to the sensors.

III. RESULTS

A. Morphology of ZnS-Doped Mn Nanomaterials and Sensing Film

The crystal structure and morphology of CH-capsulated ZnS-doped Mn nanomaterials were characterized before all the sensing experiments. The sample of CH-ZnS/Mn was taken with the XRD and SEM



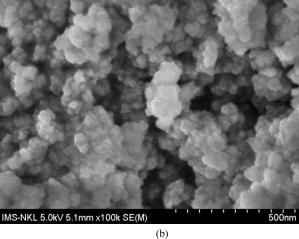


Fig. 2. (a) X-ray spectrum of Chitosan-capped ZnS-doped Mn nanograins taken by Rigaku MiniFlex600. (b) SEM image of the same sample captured by HITACHI S-4800.

in Fig. 2. In Fig. 2(a), three peaks at (111), (220), and (311) were observed. This result confirmed a cubic sphalerite structure of the materials and proved that CH-ZnS/Mn was successfully synthesized (JCPDS card No.5-0566). Because the percentage of Mn⁺² and CH is small, there is no effect on the structure of ZnS. The morphology and size of the materials were characterized by SEM images in Fig. 2(b). The SEM image in Fig. 2(b) showed the nanograins of Chitosan-capped ZnS-doped Mn with sizes less than 500 nm.

B. Direct Detection of Glucose by EIS Measurements

In our experiments, the glucose range is from 2 to 10 mM, which includes the diabetes threshold of 3.2 mM. First, the EIS data corresponding to different glucose concentrations was recorded. Then based on the record complex impedance value, the Nyquist plots of impedance Z were established. To analyze the electrochemical properties quantitatively, the impedance spectra were fit to a modified Randles equivalent circuit. The fitting process was completed using the EIS spectrum analyzer MATLAB-based program ZFITGUI developed by Dr J.-L. Dellis. This program is free and accessible from the MATLAB

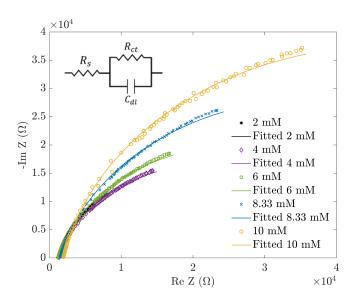


Fig. 3. Nyquist plots of impedance from the experiment (dots) and fitting process (lines) using the Randles equivalent circuit when glucose was in contact with the electrodes.

TABLE 1. Kinetic Parameters Found From the Randles Model in Fig. 3

Glucose concentrat ion (mM)	$\begin{array}{c} R_{ct} \\ (k\Omega) \end{array}$	C _{dl} (µF)	n	$R_s \ (k\Omega)$
2.00	40.8±0.8	1.85±0.03	0.86±0.02	1.17±0.01
4.00	42.3 ± 0.2	1.13 ± 0.01	0.85 ± 0.02	1.31 ± 0.01
6.00	50.5±0.4	0.95 ± 0.01	0.86 ± 0.01	1.19 ± 0.01
8.33	70.2 ± 0.1	0.65 ± 0.01	0.85 ± 0.02	1.45 ± 0.02
10.00	99.3±13.6	0.34 ± 0.02	0.87 ± 0.02	1.90±0.01

store. The fitting results and the corresponding circuit network are shown in Fig. 3. The parameters of the circuit are given in Table 1.

In Fig. 3, R_s is the solution resistance, and R_{ct} is the transfer resistance of the CH-capped ZnS-doped Mn film. $C_{\rm dl}$ is a double-layer capacitance representing the constant phase element, which reflects imperfections of the surface layer. Its value can be determined by the equation $Z = 1/(Cj\omega)^n$, where n = 0 corresponds to pure resistance, n = 1 when the constant phase element acts like an ideal capacitor C. For 0.5 < n < 1, the film is interpreted as having a nonuniform current distribution or rough [16]. At the range of studied frequency (from 10 Hz to 10 kHz), $C_{\rm dl}$ has a value from 0.34 to 1.85 μ F, and we do not observe any diffusion. Each data given in Table 1 is an average of five measurements.

The relationship between the effective resistance $1/R_{ct}$ and the glucose concentration can be approximated by the equation

$$y = -0.0187x + 0.299 \tag{1}$$

where x is the concentration of the glucose (mM), and y is inversed values of transfer resistance $R_{\rm ct}$ (see Fig. 4). Using (1), the glucose concentration level (C) can be estimated from EIS data. For deeper understanding, authors compared the working performance of glucose sensors with and without sensing film with in the range of 2–9 mM. The results pointed out that CH-ZnS/Mn helped to expand the detection range and utilize the linear working curve and confirmed that CH-ZnS/Mn is a promising sensing materials for EIS glucose sensors.

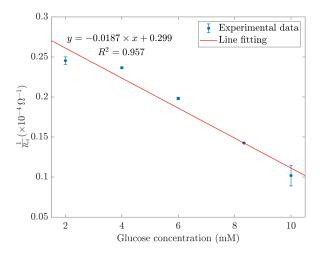


Fig. 4. Relationship between the effective resistance and the concentrations of glucose.

TABLE 2. Estimated the Concentrations of Glucose

Estimated R_{ct} $(k\Omega)$	Estimated C (mM)	Actual C (mM)	Error
40.3	2.70	3.00	10.00%
46.8	4.55	5.00	9.02%
58.9	6.88	7.14	2.62%
71.4	8.48	9.09	6.73%

In the following, to validate our method, we prepare the glucose solutions of 3, 5, 7.14, 9.09 mM and repeat the procedure described in Section II-C. The estimated values of $R_{\rm ct}$ are given in Table 2. Substituting these values into (1), we can find the concentrations of the glucose (see Table 2). Compared to the actual glucose concentrations, it is shown a high agreement between the estimated and actual values (in all cases, the differences are less than or equal to 10%).

C. Determination of the Small Signal Change

The limit of detection (LOD) is the smallest concentration of analyte the sensor can detect. When it reaches the LOD, the acquired signal does not change. Hence, the LOD is a critical parameter to knowing the efficiency of the sensor. While the analyte's concentration is low enough, the resistance change is negligible. Hence, the ability to detect this change is challenging. In this letter, we demonstrate the approach to detect the small change in the signal using the Candy algorithm [13]. This technique can enhance the sensitivity and LOD of the sensor. To illustrate the method, a small amount of glucose concentration was added to the system, and the frequency was kept constant. Hence, the complex acquired resistance is a function of time shown in Fig. 5(a). Because of the limitation of the experiment design, the smallest amount of glucose concentration can be added is 0.67 mM. In Fig. 5(a), the vertical lines indicate the change in glucose levels, which are also the sudden changes in impedance signal. In order to find these small changes in the presence of noise, first, the signal is convolved with Gaussian to filter out noise. Then, we take a derivative of the filtered signal. The result is shown in Fig. 5(b). The peaks in the derivate indicate the changes in the signal. Fig. 5 shows the agreement between the experiment and detecting results. This approach is practical for our study and other applications, such as the quartz crystal microbalance (QCM) signal or when we need to detect tiny changes in a signal.

10000

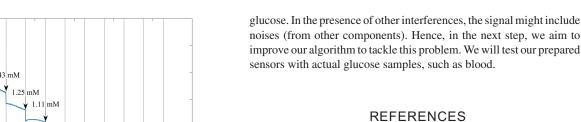
-35

0

200

400

2 mM



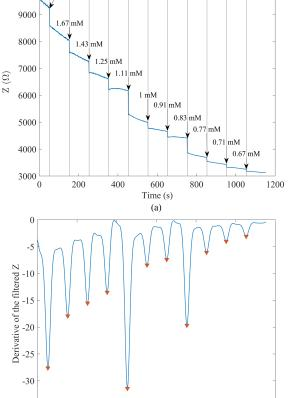


Fig. 5. (a) The impedance response of the sensor to different concentrations of glucose. (b) The derivatives of the filtered impedance response. The red peaks indicate the changes in the glucose level.

600

Time (s)

(b)

800

1000

1200

IV. CONCLUSION

In this letter, using the EIS approach, we reported the enzyme glucose sensors based on CH-capped Zn-doped Mn nanomaterials for the first time. The agreement between the experimental data and Randles fitting approach confirmed that the EIS could be an alternative method to detect glucose in a small range. This sensor is easy to prepare and operates stably. This letter also served as a technique approval for using the computer aid to enhance the LOD of many sensors. As a drawback, this algorithm is applied for the electrochemical measurements of pure

- F. Mizutani and S. Yabuki, "Rapid determination of glucose and sucrose by an amperometric glucose-sensing electrode combined with an invertase/mutarotaseattached measuring cell," *Biosensors Bioelectron.*, vol. 12, no. 9/10, pp. 1013–1020,
- [2] K. Yoshimura and K. Hozumi, "Response characteristics of a glucose electrode with a sensing membrane prepared by plasma polymerization," *Microchemical J.*, vol. 53, no. 4, pp. 404–412, 1996.
- [3] J.-J. Xu and H.-Y. Chen, "Amperometric glucose sensor based on glucose oxidase immobilized in electrochemically generated poly (ethacridine)," *Analytica Chimica Acta*, vol. 423, no. 1, pp. 101–106, 2000.
- [4] K. S. Kim, S. K. Kim, K. M. Sung, Y. W. Cho, and S. W. Park, "Management of type 2 diabetes mellitus in older adults," *Diabetes Metabo. J.*, vol. 36, no. 5, pp. 336–344, 2012
- [5] H. Teymourian, A. Barfidokht, and J. Wang, "Electrochemical glucose sensors in diabetes management: An updated review (2010–2020)," *Chem. Soc. Rev.*, vol. 49, no. 21, pp. 7671–7709, 2020.
- [6] V. B. Juska and M. E. Pemble, "A critical review of electrochemical glucose sensing: Evolution of biosensor platforms based on advanced nanosystems," Sensors, vol. 20, pp. 21–2020. Art. pp. 6013.
- [7] M. Sharma, T. Jain, S. Singh, and O. Pandey, "Tunable emission in surface passivated Mn-ZnS nanophosphors and its application for glucose sensing," AIP Adv., vol. 2, no. 1, 2012, Art. no. 012183.
- [8] S. Wang, "A fluorescent sensor based on one-step fabrication of chitosan/ZnS: Mn2+ composite film for iodine ion detection," *Mater. Technol.*, vol. 33, no. 4, pp. 271–275, 2018
- [9] C.-S. Hwang, J. Kim, and U. S. Shin, "Novel application of the chitosan-capped ZnS: Mn nanocrystals for the detection of copper (II) ions in aqueous solution," *J. Korean Phys. Soc.*, vol. 78, no. 12, pp. 1241–1248, 2021.
- [10] L. Liu, Y. Chen, H. Lv, G. Wang, X. Hu, and C. Wang, "Construction of a non-enzymatic glucose sensor based on copper nanoparticles/poly (o-phenylenediamine) nanocomposites," *J. Solid State Electrochemistry*, vol. 19, no. 3, pp. 731–738, 2015.
- [11] L. Fang et al., "Flower-like MoS2 decorated with Cu2O nanoparticles for non-enzymatic amperometric sensing of glucose," *Talanta*, vol. 167, pp. 593–599, 2017.
- [12] E. Barsoukov and J. R. Macdonald, "Impedance spectroscopy theory, experiment," in *Applications*, 2nd ed. Hoboken, NJ, USA: Wiley, 2005.
- [13] J. Canny, "A computational approach to edge detection," *IEEE Trans. Pattern Anal. Mach. Intell.*, vol. PAMI-8, no. 6, pp. 679–698, Nov. 1986.
- [14] S. Ummartyotin, N. Bunnak, J. Juntaro, M. Sain, and H. Manuspiya, "Synthesis and luminescence properties of ZnS and metal (Mn, Cu)-doped-ZnS ceramic powder," *Solid State Sci.*, vol. 14, no. 3, pp. 299–304, 2012.
- [15] A. J. Bard, J. A. Crayston, G. P. Kittlesen, T. V. Shea, and M. S. Wrighton, "Digital simulation of the measured electrochemical response of reversible redox couples at microelectrode arrays: Consequences arising from closely spaced ultramicroelectrodes," *Anal. Chem.*, vol. 58, no. 11, pp. 2321–2331, 1986.
- [16] C. Sung, "Thermal transitions in layer-by-layer assemblies," Ph.D. dissertation, Texas A&M Univ., College Station, TX, USA, 2014.